

# An Original Aspirin-Containing Carbonic Anhydrase 9 Inhibitor Overcomes Hypoxia-induced Drug Resistance to Enhance The Efficacy of Myocardial Protection

Wen Zhou (✉ [wzhou@seu.edu.cn](mailto:wzhou@seu.edu.cn))

Southeast University <https://orcid.org/0000-0001-9506-1620>

Bin Zhang

Southeast University

Keyu Fan

Southeast University

Xiaojian Yin

China Pharmaceutical University

Jinfeng Liu

China Pharmaceutical University

Shaohua Gou

Southeast University

---

## Research Article

**Keywords:** myocardial hypoxia injury, drug resistance, carbonic anhydrase 9, aspirin derivative

**Posted Date:** February 22nd, 2021

**DOI:** <https://doi.org/10.21203/rs.3.rs-216260/v1>

**License:**  This work is licensed under a Creative Commons Attribution 4.0 International License.

[Read Full License](#)

---

**Version of Record:** A version of this preprint was published at Cardiovascular Drugs and Therapy on April 12th, 2021. See the published version at <https://doi.org/10.1007/s10557-021-07182-2>.

# Abstract

**Purpose** Hypoxic microenvironment plays a vital role in myocardial ischemia injury, generally leading to the resistance of chemotherapeutic drugs. This induces an intriguing study on mechanism exploration and prodrug design to overcome the hypoxia induced drug resistance.

**Methods** In this study, we hypothesized that the overexpression of carbonic anhydrase 9 (CAIX) in myocardial cells is closely related to the drug resistance. Herein, bioinformatics analysis, gene knockdown and overexpression assay certificated the correlation between CAIX overexpression and hypoxia. An original aspirin-containing CAIX inhibitor AcAs has been developed.

**Results** Based on the downregulation of CAIX level, both in vitro and in vivo, AcAs can overcome the acquired resistance, and more effectively attenuate myocardial ischemia and hypoxia injury than that of aspirin. CAIX inhibitor is believed to recover the extracellular pH value so as to ensure the stable effect of aspirin.

**Conclusion** Results indicate great potential of CAIX inhibitor for further application in myocardial hypoxia injury therapy.

## 1. Introduction

Myocardial ischemia injury is a pressing issue which denotes the presence of heart diseases, such as coronary artery disease (CAD) and myocardial infarction (MI).<sup>1</sup> Unfortunately, cellular hypoxic microenvironment significantly limits the efficacy of most chemotherapeutic drugs, such as aspirin.<sup>2-5</sup> In fact, hypoxia induced resistance to the conventional antitumor chemotherapy has been confirmed, and great efforts have been made to develop hypoxia-specific theranostics.<sup>6,7</sup> However, this problem has not attracted much attention in the study of anti-myocardial hypoxia injury. Therefore, original target exploration and drug discovery will be of great requirement to overcome the resistance to ensure the drug efficacy.

In detail, aspirin is a classic and practical drug to prevent the occurrence of heart disease. It can inhibit platelet adhesion and aggregation, and prevent the formation of thrombus by inhibiting the generation of cyclooxygenase-1 (Cox-1) and cyclooxygenase-2 (Cox-2) coenzymes.<sup>8,9</sup> However, latest clinical statistics and studies have challenged the role of aspirin in preventing and attenuating myocardial injury. Aspirin cannot attenuate myocardial injury when ischemia and hypoxia occur.<sup>10</sup> It also has no efficacy given before blood reperfusion surgery to attenuate myocardial ischemia reperfusion injury.<sup>4,5</sup> Evidently, recent studies have called into question about the efficacy of traditional drugs under hypoxic microenvironment. So there is an urgent need to optimize traditional drugs or develop new drugs to attenuate myocardial ischemia injury.

Moreover, myocardial ischemia injury is closely related to hypoxia inducible factor-1 $\alpha$  (HIF-1 $\alpha$ ) pathway abnormality.<sup>11,12</sup> Coincidentally, carbonic anhydrase 9 (CAIX), a transmembrane protein composed of

acidic amino acids, has a HIF responsive element in its promoter region. More significantly, CAIX is also involved in regulation of *in vitro* pH. Existing researches have shown that high expression of HIF-1 $\alpha$  can upregulate the expression of downstream target gene product CAIX in tumor cells.<sup>13-16</sup> However, little attention has been paid to whether overexpression of HIF-1 $\alpha$  induces high expression of CAIX under conditions of cardiac ischemia and cardiomyocyte hypoxia as well. Up till now, the association between myocardial ischemia injury and abnormal CAIX expression is rarely reported. In fact, CAIX is expressed not only in tumor cells, but also in the mammalian heart,<sup>17, 18</sup> localizing to the t-tubules of cardiomyocytes.<sup>19</sup> In view of the similar hypoxic microenvironment between tumor cells and hypoxic cardiomyocytes, the role of CAIX in myocardial hypoxia injury will be a meaningful exploration. Inhibiting CAIX overexpression to regulate the abnormal acidic microenvironment *in vivo* will probably be a new and promising strategy to overcome the hypoxia induced drug resistance and can effectively attenuate myocardial ischemia injury.

In this study, carbonic anhydrase isozymes were searched and analyzed using the protein database Uniprot, Bgee, String and Pathway Commons Search. The expression levels of different isoenzymes in the heart were compared and the expression of CAIX in heart tissues was clarified. The protein interactions between CAIX and HIF-1 $\alpha$  were confirmed. We further certified that HIF-1 $\alpha$  regulates the CAIX expression level in cardiomyocytes through experiments such as PA simulation hypoxia modeling, gene knockdown and overexpression. To prove the improvement effect of CAIX inhibition on drug efficacy, we designed and prepared a novel compound AcAs containing both aspirin and acetazolamide species in a molecular entity. Since acetazolamide is a classic CAIX inhibitor,<sup>20</sup> we attempt to regulate the abnormal acidic extracellular microenvironment by inhibiting CAIX overexpression during hypoxia, thereby reducing the hydrolysis of ester bonding drugs like aspirin. In order to verify the effect of AcAs on attenuating myocardial hypoxic injury, the cardiac myocytes hypoxia model and the mice ischemia model were set up. The enhancing efficacy of AcAs on myocardial protection under hypoxic microenvironment through the regulation of CAIX overexpression and extracellular pH values has been profoundly studied. Results demonstrate that under hypoxic microenvironment, AcAs can attenuate myocardial injury more effectively than aspirin. Molecular structure optimization based on CAIX inhibition is a feasible method to improve the treatment of myocardial hypoxia injury.

## 2. Results

### 2.1 CAIX Distributs in the Heart and Interacts with HIF-1 $\alpha$

From the UniProt database, we found that carbonic anhydrase (CA) has 15 isoenzymes (homo sapiens). They have a common catalytic function, reversible hydration of carbon dioxide and participation in extracellular pH adjustment. However, there are differences in the molecular structure, physical and chemical properties, immunological properties, and tissue and organ distribution of isoenzymes. We have further analyzed them through Bgee, String and Pathway Commons. Data from Bgee database show that all isoenzymes of CA except CA7 have different levels of distribution in the heart. The CAIX (CA9) gene expression score is 74.4, and the gene expression level is moderate (Fig. 1A). In the Pathway Commons

analysis, among the 15 CA isozymes, only CAIX (CA9) interacts with HIF-1 $\alpha$  (Fig. 1B). In the analysis of String protein interaction, only CAIX (CA9) interacts with HIF-1 $\alpha$ . As an upstream gene, HIF-1 $\alpha$  can regulate the expression level of CAIX (CA9) (Fig. 1C).

## 2.2 Upstream Protein HIF-1 $\alpha$ Regulates CAIX Expression in Myocardial Cells

To analyze the correlation between HIF-1 $\alpha$  and CAIX expression in myocardial cells, we used palmitic acid (PA) in different concentrations to simulate hypoxia in H9c2 cells. As Fig. 2A shows, with the increase of PA concentration (0–100  $\mu$ M), the expression of HIF-1 $\alpha$  gradually increased, indicating the feasibility of PA to simulate hypoxia modeling. At the same time, the expression of CAIX showed the same increasing trend as HIF-1 $\alpha$  had, which showed the correlation between CAIX and HIF-1 $\alpha$ . Furthermore, specific siRNA was used to silence HIF-1 $\alpha$  expression of H9c2 cells. As shown in Fig. 2B, HIF-1 $\alpha$  knockdown diminished CAIX expression. Moreover, after knocking down HIF-1 $\alpha$ , it was observed that PA stimulation did not cause up regulation of CAIX expression. In contrast, in Fig. 2C, overexpression of HIF-1 $\alpha$  in H9c2 cells transfected with plasmid pcDNA3.1-HIF-1 $\alpha$  enhanced CAIX expression, indicating that myocardial CAIX protein expression was regulated by HIF-1 $\alpha$ .

## 2.3 Synthesis of the Target Compound Containing Aspirin and Acetazolamide Units

The target compound AcAs containing aspirin (As) and acetazolamide (Ac) was prepared by the synthetic way illustrated in Fig. 3, with purity > 95% as determined by HPLC. The molecular structure of AcAs was characterized by  $^1$ H-NMR,  $^{13}$ C-NMR and ESI/TOF MS. All characterization results indicate that the target compound AcAs coincides with the structure as designed (Fig. S2-S8, Table S1).

## 2.4 AcAs Attenuates Hypoxia Injury of Cardiomyocytes More Effectively than Aspirin

With CCK8 assay, the cell viability was calculated as a ratio of the experiment hole absorbance at 450 nm to that of the control hole. It has been proved by UV spectrophotometer that the compound has no absorbance at 450 nm (Fig. S1). After dosing and hypoxia treatment, CCK8 detection showed cell viability changed with varying degrees. Under normal oxygen condition (21% O $_2$ ), AcAs and Ac&As (a combined use of Ac and As) could enhance the cell proliferation rate and improve the activity of cardiomyocytes as well as As, while Ac did not (Fig. 4A). Intriguingly, under hypoxic conditions (1% O $_2$ ), the effect of As was weakened remarkably, while AcAs and Ac&As had a better effect, and AcAs even showed increasing cell proliferation rate obviously at low concentrations (Fig. 4B).

The cell membrane integrities of different groups were examined by flow cytometry using Hoechst 33342 and Propidium Iodide (PI) double staining. Hoechst 33342 (bisBenzimide H33342) is a blue fluorescent dye which can penetrate cell membrane. When the cell undergoes apoptosis, the chromatin shrinks, and the fluorescence of the apoptotic cell will be significantly enhanced after staining. PI cannot penetrate cell membranes, and cannot stain normal cells or viable apoptotic cells with intact cell membranes. For necrotic cells and late apoptotic cells, the integrity of the cell membrane is lost, and PI can stain the necrotic cells. This distinguishes normal cells, apoptotic cells and necrotic cells. As shown in Fig. 4C, cells

in the blank group were almost completely normal cells (located at Hoechst 33342-/PI-), and the necrotic cells and late apoptotic cells in the model group were significantly increased to 14.02% (located at Hoechst 33342+/PI+), indicating that hypoxia stimulation could easily lead to late apoptosis and programmed cell necrosis. In the medicated group, necrotic cells and late apoptotic cells were reduced at different levels, 10.64%, 7.87%, 5.13%, 3.51% of As, Ac, Ac&As and AcAs medicated groups, respectively. The results indicate that AcAs can most effectively resist cell apoptosis and necrosis caused by hypoxia.

Under hypoxic conditions, perturbation in electron transport is associated with leakage of electrons from the respiratory chain, resulting in increased ROS that could lead to myocardial hypoxia oxidative injury.<sup>21</sup> Results from the flow cytometry (Fig. 4D) indicate that hypoxic treatment can lead to a significant increase of ROS level. Distinctly, 10  $\mu$ M of AcAs and Ac&As could effectively reduce the production of ROS, while As had no effect on ROS reduction at the same concentration. In this study, ROS level is proportional to DHE oxide's fluorescence intensity. The fluorescence emission spectra of DHE oxide can be detected by fluorescence spectrophotometer (Fs, Fig. 4E), and the peak intensity variation trend of DHE oxide is consistent with the flow cytometry data.

The comparison of ATP levels in different groups is shown in Fig. 4F. Results indicate that hypoxia treatment by tri-gas incubator can reduce ATP level. 10  $\mu$ M AcAs is capable of restoring ATP level, more distinctly than that of Ac, As or Ac&As.

In brief, under hypoxia conditions, compared with Ac&As, Ac and As, AcAs can best inhibit cell apoptosis and necrosis, restore cell vitality and regulate abnormal ROS and ATP levels.

## 2.5 AcAs Works by Acting on CAIX

As shown in Fig. 5A, hypoxia modelling enhances CAIX protein expression in H9c2 cells. Both Ac and AcAs (10  $\mu$ M) reduced CAIX expression, but As did not. Further study showed that the regulation effect of AcAs (0.01–10  $\mu$ M) on CAIX expression was concentration dependent (Fig. 5B).

As Fig. 5C shows, pHe value of H9c2 cells under hypoxia (1% O<sub>2</sub>) is lower when compared with normoxia (21% O<sub>2</sub>) cultured H9c2 cells, indicating that there is a positive correlation between extracellular acidification and O<sub>2</sub> levels. In Ac and AcAs medicated group, the pHe values are increased by about 0.15, similar to the case of a CAIX inhibitor SLC-0111 (50  $\mu$ M, 1h) treatment, indicating that both Ac and AcAs can weaken extracellular acidification via the inhibition of CAIX overexpression. The pHe values are unaffected by As with the same condition.

To predict the interaction between CAIX and molecules, computer simulation was preliminarily operated. As Fig. 5D shows, AcAs inserts in the pocket surrounded by four amino acid residues Thr200, Gln92, Thr69, Gln67 with hydrogen bonds. The binding energy is -5.76 kcal/mol. Meanwhile, Ac inserts in the same pocket surrounded by three amino acid residues Thr200, Thr199, and His119 with hydrogen bonds. The binding energy is -6.0 kcal/mol. The results indicate that the binding sites and modes of AcAs and Ac to CAIX are similar, both AcAs and Ac binds to the same amino acid residue Thr200. The original

compound AcAs can bind to CAIX as stable as that of Ac. The PDB files of homology (Docking) models were listed in Table S3.

## 2.6 AcAs Attenuates Mouse Myocardial Ischemia Injury More Efficiently than Aspirin

In Fig. 6A, macroscopic enzyme mapping assay (triphenyltetrazolium chloride, TTC test) is depicted to detect the myocardial changes in the mice heart of blank and medicated groups. A high percentage of mean infarct size with increased staining was observed in isoproterenol (ISO) administered mice when compared to blank group. 20 mg/kg AcAs pretreated mice showed a moderately lower infarct size with reduced staining when compared to 85 mg/kg ISO administered mice. Administration of 20 mg/kg As had less conspicuous effect on heart tissue.

In Fig. 6B, the approximately normal morphology and structure of myocardial cells and tissues are shown in the blank group by hematoxylin-eosin (HE) staining. Myocardial tissues from ISO induced mice show the disturbance of myocardial structure, extensive edema and multiple cell boundaries blurred. The pathological injury of myocardium was alleviated in As-treated and AcAs-treated group to varying degrees. In comparison with the effect of As group, the disordered structure in AcAs group was greatly reduced, and the cell edema was much significantly improved with clearer cell boundaries.

The CAIX protein expression in myocardial tissues of different groups was measured using immunohistochemistry assay (IHC). The percentage of positive cells under the microscope and the positive staining intensity were scored and compared respectively. The positive grade was obtained by multiplying them. The higher the score is, the stronger the positive is. Compared with the blank group, the CAIX level in ISO induced model group was enhanced nearly three times. The overexpression of CAIX was not affected by Ac but substantially suppressed after AcAs treatment (Fig. 6C).

As shown in Fig. 6D, ISO modeling can enhance CAIX protein expression in myocardial tissues. AcAs (20 mg/kg) reduced CAIX expression, while As did not. These are in consistent with the results at cellular level.

The creatine kinase MB (CK-MB) and cardiac troponin (cTNI) level of the blank and ISO treated groups with or without drugs were detected. The CK-MB and cTNI level in the model group were significantly increased greater than that of the blank group. As checked by two commonly used markers of myocardial injury, the myocardial injury happened in the model group tissue, whereas in the medicated group, AcAs was found to effectively attenuate myocardial injury when compared with As (Table 1).

## 3. Discussion And Conclusions

In this research, we have made original discoveries about the CAIX expression in myocardial ischemia and hypoxia injury. By searching the protein databases, we found that CAIX is normally expressed in the heart (Fig. 1A). Among the isoenzymes of carbonic anhydrase (CA), only CAIX has a protein-protein interaction with HIF-1 $\alpha$  (Fig. 1B, 1C). Although there is an interaction between them, due to the common

hypoxic microenvironment in tumors, CAIX is currently only considered to be highly expressed in hypoxic tumor cells. Despite CAIX is a confirmed specific marker of tumorigenesis, there is a lack of systematic research on CAIX related mechanism of myocardial hypoxic injury. In view of the similar hypoxic microenvironment between tumor cells and myocardial cells, the relevant mechanism of CAIX in myocardial hypoxia injury is worthy of further investigation.

The correlation between CAIX and HIF-1 $\alpha$  in hypoxia cardiomyocytes was studied in detail. By gradient modeling of simulated hypoxia (Fig. 2A), HIF-1 $\alpha$  knockdown (Fig. 2B) and overexpression assay (Fig. 2C), the results jointly revealed that CAIX is overexpressed in hypoxic cardiomyocytes, and CAIX expression is depended on HIF-1 $\alpha$  related pathways. The inhibition of CAIX overexpression is expected to be an effective strategy to overcome the drug resistance due to hypoxia, and better attenuate myocardial hypoxic injury. In order to verify whether the regulation of CAIX overexpression could attenuate myocardial injury, we not only selected well-known CAIX inhibitor acetazolamide (Ac) for verification, but also designed a brand-new compound AcAs for exploration (Fig. 3). We connected the CAIX inhibitor Ac to the classic cardioprotective drug aspirin (As) in a molecular entity so as to obtain a kind of potential drug with enhancing efficacy.

Our study indicates that AcAs has obvious advantages in improving cell proliferation, especially under hypoxic microenvironment (Fig. 4A, 4B), reducing cell necrosis (Fig. 4C), decreasing ROS level (Fig. 4D, 4E), and increasing ATP level (Fig. 4F). By comparing the efficacy between As and AcAs, we found that at cellular level, AcAs can better downregulate CAIX overexpression (Fig. 5A, 5B). Both Ac and AcAs could bind with CAIX around the active site (Fig. 5D). In mouse experiments, both TTC (Fig. 6A), HE (Fig. 6B) assay showed that AcAs could better attenuate ISO induced myocardial ischemia injury than As. In IHC (Fig. 6C) and WB (Fig. 6D) assay we found that CAIX level in mice heart can be downregulated by AcAs. Moreover, creatine kinase MB isoenzyme (CK-MB) and cardiac troponin I (cTNI) are two important indicators to diagnose myocardial injury through detecting enzyme levels in serum. The effect of AcAs to reduce CK-MB activity and cTNI level was greater than that of As (Table 1). The results have verified our idea of CAIX inhibitors for myocardial injury protection and provided a promise for the research and development of new myocardial injury protection drugs targeting CAIX.

In view of the role of CAIX in cells, we explored the mechanism by which compounds optimized by CAIX inhibitor could effectively attenuate myocardial injury under hypoxic microenvironment. CAIX catalyzes the reversible hydration of CO<sub>2</sub> in cells and makes conversion of CO<sub>2</sub> into bicarbonate, resulting in promoting the transfer and discharge of CO<sub>2</sub>, and maintaining the acid-base balance. When the CAIX protein is overexpressed, CO<sub>2</sub> will be excessively excreted, and HCO<sub>3</sub><sup>-</sup> will increase significantly, resulting in an enhanced extracellular acidic environment. Aspirin has an ester bond that is prone to hydrolysis when the acidity is increased. The inhibition of CAIX overexpression is expected to recover the normal extracellular pH value and ensure that aspirin exerts a stable effect. By testing and comparing the extracellular pH variations of cardiomyocytes in the blank, hypoxic model and medicated groups (Fig. 5C), we found that the pH value in the hypoxic model group was significantly reduced, which was consistent with the result of CAIX overexpression in the model group. The AcAs medicated group was

found to effectively regulate abnormal acidity, proving that CAIX inhibition regulates the extracellular pH values to overcome the drug resistance due to hypoxia.

In summary, the association between myocardial ischemia injury and CAIX overexpression has been confirmed. An original aspirin-containing CAIX inhibitor was designed and synthesized to validate our hypothesis. The experimental results of the drug efficacy at cell and animal levels confirmed that down-regulation of CAIX overexpression is an absolutely new strategy to effectively attenuate myocardial ischemia injury. Such an approach is able to overcome the drug resistance due to hypoxia. More intriguingly, we have explicated that CAIX inhibitors can regulate the abnormal extracellular acidity to ensure the drug stability. In all, our work on the application of CAIX offers a promising strategy for drug design aiming at myocardial ischemia and hypoxia injury treatment.

## 4. Experimental Section

### 4.1 Protein Distribution of Carbonic Anhydrase Isoenzymes in the Heart and Protein-Protein Interaction Analysis

CAIX is one of carbonic anhydrase isoenzymes. Isoenzymes have the same catalytic function, but there are differences in immunological properties, tissue and organ distribution among them. We searched and compared with these isoenzymes by various databases. The databases include Uniprot Database (<https://www.uniprot.org>), Bgee Database (<https://bgee.org>), Pathway Commons Database (<http://apps.pathwaycommons.org>), String Database (<https://string-db.org>). The Universal Protein Resource (UniProt) is a comprehensive resource for protein sequence and annotation data. Bgee is a database to retrieve and compare gene expression patterns in multiple animal species based exclusively on curated "normal", healthy, expression data. This allows comparisons of expression patterns between species. Pathway Commons is an access to biological pathway information collected from public pathway databases. String is a database of known and predicted protein-protein interactions. The interactions include direct (physical) and indirect (functional) associations; they stem from computational prediction, from knowledge transfer between organisms, and from interactions aggregated from other (primary) databases.<sup>22</sup>

### 4.2 Palmitic Acid (PA) Simulated Hypoxia Modeling

The variation trend of HIF-1 $\alpha$  and CAIX protein expression was studied by western blot (WB). The correlation between myocardial CAIX and HIF-1 $\alpha$  could be found. In detail, H9c2 cell hypoxia model was simulated by PA with different concentrations (0–100  $\mu$ M). Protein was extracted from cells with ice-cold radioimmunoprecipitation assay (RIPA) buffer containing 1 mmol/L phenylmethanesulfonyl fluoride (PMSF). The lysates were centrifuged at 12000 g for 15 min at 4 °C. The protein concentration was quantified by Bicinchoninic Acid Protein Assay kit (Biosky Biotechnology Corporation, Nanjing, China). Western blot assay was used for protein expression analysis with primary antibody (anti-HIF-1 $\alpha$ , proteintech, 1:500, 20960-1-AP; anti-CAIX, proteintech, 1:500, 11071-1-AP; anti-GAPDH, Bioworld

Technology, 1:500, AP0063) and HRP-conjugated secondary antibody (Goat Anti-Rabbit IgG (H+L) HRP, 1:3000, Bioworld Technology, BS13278, or Rabbit Anti-Goat IgG (H+L)-HRP, 1:3000, Bioworld Technology, BS30503). Equal loading was verified by incubation with anti-GAPDH. The blots were visualized using ECL, and the signals were quantified by densitometry (Image-Pro Plus 6.0).

### 4.3 HIF-1 $\alpha$ siRNA Transfection

H9c2 cells were transfected with HIF-1 $\alpha$  siRNA (sc-45919) (Santa Cruz, CA, USA) in 6-well plates using siRNA transfection reagent (sc-29528) (Santa Cruz). 1 mL pre-diluted mixture containing siRNA (HIF-1 $\alpha$ ) and transfection reagent was incubated at 37 °C for 5–7h, and the culture was continued for 48h with twice liquid exchange. Some transfection groups were subjected to 100  $\mu$ mol/L palmitic acid (PA) for additional 2h. The cell proteins were obtained for WB analysis to analyze HIF-1 $\alpha$  and CAIX expressions. The detailed WB method was the same as in 4.2.

### 4.4 Overexpression Plasmid Construction

H9c2 cells were transfected with pcDNA3.1-HIF-1 $\alpha$  (GenePharma, Shanghai, China) in 6-well plates using Hieff Trans™ Liposomal Transfection Reagent (Yeasen, Shanghai, China). pcDNA3.1-HIF-1 $\alpha$  and transfection reagent were mixed and incubated at r.t. for 20 min to form a complex of DNA-liposomes. The mixed solution was added to each well of the cell culture plate, and after continuous culture for 48h, the cell proteins in each group were extracted. WB assay was performed to determine the protein expression level and the correlation between HIF-1 $\alpha$  and CAIX. The detailed WB method was the same as in 4.2.

### 4.5 Synthesis of Compound AcAs

Reagents for compound synthesis such as acetazolamide (Ac), aspirin (As), 6-heptyl acetylenic acid, 2-bromine ethanol, triethylamine, sodium azide, copper acetate, ascorbic acid, concentrated hydrochloric acid, sodium bicarbonate were of analytical grade and used without further purification. <sup>1</sup>H-NMR spectra were performed on a Bruker 600 MHz Ultra shield spectrometer (Avance Av-500) and reported as parts per million (ppm) from TMS. The final product AcAs was also characterized by 150 MHz <sup>13</sup>C-NMR spectra. High-resolution mass spectrum was measured by an Agilent 6224 ESI/TOF MS instrument.

The compound was prepared as follows.

5-Amino-1,3,4-thiadiazole-2-sulfonamide (Intermediate 2): To a solution of acetazolamide (22.5 mM, 5.0 g) in ethanol (30 mL), concentrated hydrochloric acid (5 mL) was added at room temperature, then the mixture was kept stirring and refluxing until the reaction completed. After the solution was concentrated in vacuum, a small amount of saturated sodium bicarbonate solution was added to adjust pH=9. The resulting solution was extracted by ethyl acetate, and the organic phase was concentrated to produce white powder. Yield: 3.5g, 86.4 %. <sup>1</sup>H NMR (600 MHz, DMSO-d<sub>6</sub>)  $\delta$  8.06 (s, 2H), 7.81 (s, 2H).

N-(5-Sulfamoyl-1,3,4-thiadiazol-2-yl)hept-6-ynamide (Intermediate 3): Under ice bath, 2 eq oxaloyl chloride and a drop of DMF was added to a solution of 6-heptylic acid (277 mg) in dichloromethane (DCM) (6 mL). After stirring for 6–8 h, it was concentrated to remove DCM by a rota-vapour. Intermediate 2 (360 mg) and pyridine (316 mg) were dissolved in DMF (5 mL) under ice bath, then the above 6-heptylenyl chloride in DMF was added for reaction which was monitored by TLC. The solution was concentrated in vacuum and the residue was isolated by silica gel column chromatography (DCM: MeOH= 40:1, V:V). The product was obtained as white powder. Yield: 0.42g, 73.7%. <sup>1</sup>H NMR (600 MHz, DMSO-d<sub>6</sub>) δ 13.0 (s, 1H), 8.32 (s, 2H), 2.78 (t, J = 2.4 Hz, 1H), 2.55 (t, J = 7.2 Hz, 2H), 2.20–2.17 (m, 2H), 1.73–1.68 (m, 2H), 1.50–1.45 (m, 2H).

2-Bromoethyl 2-acetoxybenzoate (Intermediate 5): Aspirin (360 mg), 2 eq oxaloyl chloride and a drop of DMF were mixed in DCM (6 mL) in an ice bath. The mixture was kept stirring for 6–8 h, then DCM was removed by a rota-vapour. To a solution of 2-bromoethanol (250 mg) and trimethylamine (303 mg) in DCM (6 mL) in an ice bath the above solution of aspirinyl chloride was added. The reaction continued stirring at 0 °C for 6 h, DCM was used for extraction, the resulting organic phase was concentrated in vacuum and the residue was isolated by silica gel column chromatography (petroleum ether: ethyl acetate = 8:1, V:V) to obtain yellow oil. Yield: 0.40 g, 70.2 %.

2-Azidoethyl 2-acetoxybenzoate (Intermediate 6): A mixture of intermediate 5 and NaN<sub>3</sub> (130 mg) in DMF (6 mL) was heated to 50 °C and kept stirring overnight. The solution was concentrated and the resulting residue was isolated by silica gel column chromatography to get yellow oil. Yield: 190 mg, 76.3%. <sup>1</sup>H NMR (600 MHz, CDCl<sub>3</sub>) δ 8.04 (d, J = 7.8 Hz, 1H), 7.58 (t, J = 7.8 Hz, 1H), 7.33 (t, J = 7.8 Hz, 1H), 7.12 (d, J = 7.8 Hz, 1H), 4.43 (d, J = 4.8 Hz, 1H), 3.59 (d, J = 4.8 Hz, 1H), 2.37 (s, 3H).

Compound AcAs: To a stirring solution of intermediate 3 (60 mg) in methanol (8 mL) copper acetate (8 mg) and intermediate 6 (52 mg) were subsequently added. 15 mg of ascorbic acid was added 5 min later. The reaction maintained stirring for 4h, then the solution was concentrated, white solid powder was obtained by silica gel column chromatography. Yield: 80 mg, 71.4%. Purity is 98.9% detected by HPLC. <sup>1</sup>H NMR (600 MHz, DMSO-d<sub>6</sub>) δ 13.00 (s, 1H), 8.32 (s, 2H), 7.93 (s, 1H), 7.82 (d, J = 6.9 Hz, 1H), 7.69–7.60 (m, 1H), 7.42–7.32 (m, 1H), 7.21 (d, J = 7.6 Hz, 1H), 4.69 (s, 2H), 4.61 (s, 2H), 2.69–2.59 (m, 2H), 2.59–2.50 (m, 2H), 2.20 (s, 3H), 1.70–1.54 (m, 4H). <sup>13</sup>C NMR (150 MHz, DMSO-d<sub>6</sub>) δ 172.19, 169.10, 164.26, 163.40, 161.13, 150.16, 146.66, 134.52, 131.16, 126.24, 124.10, 122.50, 122.34, 63.27, 48.28, 34.55, 28.35, 24.67, 23.92, 20.65. Ms: Found m/z: 538.11157 (calculated for C<sub>20</sub>H<sub>23</sub>N<sub>7</sub>O<sub>7</sub>S<sub>2</sub>, 537.1).

## 4.6 Cell Culture and Modelling

Cardiac myoblasts H9c2 were cultured in Dulbecco's Minimum Essential Medium (DMEM) containing 10% fetal bovine serum (FBS). Meanwhile, Primary cultured neonatal rat myocardial cells were used in some experiments. These cells were extracted from the hearts of 10 neonatal rats born 1-2 days old and cultured with DMEM containing 10% FBS. Blank group cells were common cultured under normal oxygen. Model group cells were cultured under hypoxia or given simulated hypoxia modeling reagent palmitic

acid (PA). For hypoxia treatment, cells were starved 2h in DMEM without FBS and glucose in cell incubator (37 °C, 21% O<sub>2</sub>, 5% CO<sub>2</sub>), treated with or without drugs (10 μm) for 2h and finally subjected to hypoxia conditions (37 °C, 1% O<sub>2</sub>, 5% CO<sub>2</sub>) for 4h, then cells were placed on ice to stop the cell activities. It has been reported that PA oxidation leads to local hypoxia in myocardial cells, so PA can be used as a simulated hypoxia modeling agent.<sup>23</sup> 0.0513g PA was dissolved in 1 ml anhydrous ethanol to get 200 mM mother liquor, which was diluted at 1:19 (10% BSA) to 10 mM working liquor and further diluted 100 times to 100 μM as modeling reagent.

#### **4.7 Cell proliferation Assay**

Primary cultured neonatal rat myocardial cells were used. After cells culturing with aspirin (As), acetazolamide (Ac), AcAs or a combined use of Ac and As (Ac&As) under hypoxia or normoxia treatment, cell proliferation was detected with Cell Counting Kit-8 (CCK-8, Beyotime Institute of Biotechnology, Shanghai, China). The CCK-8 kit contains 2-(2-methoxy-4-nitrophenyl)-3-(4-nitrophenyl)-5-(2,4-disulfophenyl)-2H-tetrazoliumsodiumsalt (WST-8). In the presence of the electron carrier 1-methoxy phenazine methosulfate (1-methoxy PMS), WST-8 is reduced by intracellular dehydrogenase to generate water-soluble orange-yellow formazan which can be dissolved in the tissue culture medium, and the amount of formazan is proportional to the number of living cells.<sup>24</sup> Cells were harvested and stained in a microplate with 96 wells with working solution WST-8. The absorbance intensity at 450 nm was measured with a microplate reader. We calculated the ratio of the absorbance value between the administration group and the blank control group for graphical analysis.

#### **4.8 Cell Membrane Integrity Assay**

The integrity of cell membrane can be used to distinguish normal cells from necrosis. In this study, apoptosis and necrosis assay kit was used to detect the improvement effect of aspirin (As), acetazolamide (Ac), AcAs or a combined use of Ac and As (Ac&As) on apoptosis or necrosis caused by hypoxia. H9c2 cells were cultured in a six-well plate overnight. After the cells adhered, As, Ac, AcAs (10 μmol/L) or Ac&As (10 μmol/L each for Ac and As) were added, respectively, and then incubated for 4h under hypoxia condition. Cells were washed with PBS for 3 times and resuspended in 1 mL cell staining buffer, added Hoechst 33342 (5 μL), PI (5 μL) and incubated at 4 °C for 30 minutes, and then detected by flow cytometry. The results of cell double staining test were analyzed with FCS Express V3 software.

#### **4.9 ROS Level**

DCFH-DA was used as a fluorescent probe to detect the content of ROS in cells. DCFH-DA is not fluorescent. It easily penetrates into the cell, and is hydrolyzed to DCFH by the esterase. Non-fluorescent DCFH can no longer penetrate the cell membrane, so DCFH-DA is easily load fluorescence probe. ROS in cells can oxidize DCFH to fluorescent DCF, and the fluorescence intensity can indicate the level of ROS content in cells. Cell grouping and drug administration methods were the same as described in 4.8. DCFH-DA was added into DMEM (containing 10% FBS) to incubate for at least 30 min. ROS level was then detected by fluorescence spectrophotometer and flow cytometry.

#### 4.10 ATP Level

ATP production was measured using ATP Assay Kit (Beyotime Institute of Biotechnology, Shanghai, China), according to the manufacturer's instructions. The kit is based on the fact that firefly luciferase catalyzes the fluorescence production of fluorescein, which requires ATP to provide energy, and the fluorescence is proportional to the concentration of ATP, thereby detecting ATP concentration.<sup>24</sup> After hypoxia treatment, the culture dish was placed on ice rapidly, and all metabolic activities of the cells were stopped. The culture solution was aspirated and the cell lysate was added, cell lysis solution was collected, centrifuged at 12000 g for 5 min under 4 °C, and the supernatant was taken for detection. The RLU value (The fluorescence intensity) was measured by fluorescence spectrophotometer. Solutions were evaluated in triplicate.

#### 4.11 Western Blot to Study the Interaction between Compounds and CAIX

After hypoxia or normoxia cell culture with aspirin (As), acetazolamide (Ac) or AcAs, CAIX expression level in myocardial cells was studied by WB assay. The detailed WB method was the same as in 4.2.

#### 4.12 Extracellular pH Regulation by Compounds

The cells were inoculated at the density of  $1 \times 10^5$  cells/well in a 24-well plate. After cells were attached to the well, the supermatamt was replaced with DMED containing compounds and incubated in a normoxic (21% O<sub>2</sub>) or hypoxic (1% O<sub>2</sub>) incubator. At the beginning and end of each experiment, we inserted the pH probe into the medium to measure the extracellular pH and  $\Delta$ pH was calculated. 3 replicate wells were set for each group.

#### 4.13 Docking

Molecular modelling was operated to exhibit the detail binding mode between the compounds and CAIX by docking program AutoDock 4.2.6.<sup>25, 26</sup> The 3D structure of CAIX (PDB ID: 6FE2) was downloaded from NCBI database (<http://www.ncbi.nlm.nih.gov/>). The structure of compounds AcAs and acetazolamide was extracted from Chem3D Ultra Pro 14.0 (Table S3). The size of the docking box was 60 Å × 60 Å × 60 Å, which was centered at the enzyme active pocket. The dimension grid box with a certain grid spacing (0.375 Å) was large enough to enclose the active pocket. The protein structure was kept fixed during molecular docking. For each complex, the top ranked docking pose was optimized in the binding pocket, and then used as the geometry for the binding mode analysis. All the water molecules except coordinated water were removed and charges were assigned to the molecule file. The remaining genetic algorithm (GA) parameters were set as default values, except the genetic algorithm adjusted to run at 100.<sup>27</sup>

#### 4.14 Myocardial Ischemia Injury Mouse Modeling and Evaluation of Drug Efficacy

Kunming male mice (4–6 weeks) were purchased from Shanghai Jiesijie Laboratory Animal Co., LTD. The animal care and experimental procedures were approved by Animal Ethics Committee of Southeast

University (0990200).

Male Kunming mice were randomly divided into four groups, six in each group, respectively Blank group (normal feeding), Model group (ISO modeling), two Medicated groups (20 mg/kg As or AcAs and ISO). The hypoxia modeling method was as follows: In the pre-experimental stage, both high and low concentrations were used for modelling, results showed that 20 mg/kg continuous administration for three days could not cause significant myocardial hypoxia injury, and 85mg/kg showed obvious effect. 85 mg/kg isoproterenol (ISO) was injected subcutaneously once a day for three consecutive days. ISO is a  $\beta$ -adrenergic agonist that could induce severe stress to cardiomyocyte, which can lead to the loss of myocardial integrity through oxygen deficit.<sup>28</sup> ISO-induced myocardial injury serves as a well standardized model to study the beneficial effects of drugs and cardiac function.<sup>29</sup> In the blank group, an equal amount of 0.5% sodium carboxymethyl cellulose was injected. In the medicated groups, drugs were given 20 mg/kg 2h before the injection of ISO. After the ISO injection on the third day for 1h, the mice were sacrificed by cervical dislocation method. The heart was quickly removed after the euthanasia, detected by TTC and HE staining, or stored at  $-80^{\circ}\text{C}$  for subsequent western blot experiments, or placed in 4% paraformaldehyde for Immunohistochemical (IHC) detection. Myocardial tissue protein was extracted for WB detection. Blood was taken for the detection of myocardial enzymes.

#### **4.15 TTC Staining of the Mouse Heart**

The mice hearts were isolated followed by 1% triphenyltetrazolium chloride (TTC) staining to test infarct size. TTC is a proton receptor of the pyridine-nucleoside structure enzyme system in the respiratory chain. It reacts with dehydrogenases in normal tissues and turns red, while dehydrogenase activity in ischemic tissues decreases and turns white. The heart was washed by PBS and cut into 5 pieces, and then stained in TTC solution with a water bath at  $37^{\circ}\text{C}$  for 15–30 min. Pictures were taken under the microscope to calculate the percentage of myocardial infarction area.

#### **4.16 HE Staining of the Mouse Heart**

Hematoxylin-eosin (HE) staining was used to observe the pathological changes of myocardial tissue. The hearts of mice were fixed by soaking in 4% paraformaldehyde, and paraffin sections were prepared for staining. They were observed by light microscope and images were collected for analysis.

#### **4.17 IHC Assay of the Mouse Heart**

The mouse hearts of each group were isolated and fixed with 4% paraformaldehyde. After dehydration, the hearts were embedded in paraffin and sliced. The slices were pasted on glass slides and put in the fixative. After blocking with 3% peroxy methanol for 25 min at r.t., the primary antibody (anti-HIF-1-inhibitor, proteintech, 1:50, 20960-1-AP; anti-CAIX, proteintech, 1:50, 11071-1-AP) was added to incubate overnight at  $4^{\circ}\text{C}$ , then incubated with HRP-labeled broad-spectrum secondary antibody for 1h at r.t.. The nucleus was stained with DAPI. After dehydration stabilized, the staining was detected with NanoZoomer 2.0-RS (Hamamatsu, Japan).

#### 4.18 WB Assay of the Myocardial Tissue Protein

Myocardial tissue protein preparation: After the end of the perfusion experiment, quickly remove the heart, cut out the ventricular tissue, weigh a certain amount of tissue and cut it, and add the lysate containing the protease inhibitor at a ratio of 1:9 (mg:μL). Grind on ice for 40 times using a glass homogenizer. The homogenate was collected, centrifuged at 12000 rpm for 15 min at 4 °C, and the supernatant was collected. A small amount of the supernatant was collected for protein quantification according to the BCA protein content determination kit. Add the remaining supernatant to 1/2 volume of 6× loading buffer, mix well, boil in boiling water for 10 min, cool it for WB detection, or put it in -80 °C refrigerator for future use.

#### 4.19 Myocardial Enzyme Level in Mouse Serum

Creatine kinase MB isoenzyme (CK-MB) is one of the most important indicators of diagnosing myocardial injury through detecting enzyme levels in serum. Cardiac troponin I (cTNI) is a specific antigen of cardiomyocytes, which is degraded from the myocardial fiber when the cardiomyocytes are injured, and the content significantly increases. cTNI is another marker of myocardial injury. The contents of CK-MB and cTNI were detected by the corresponding kit and the automatic biochemical instrument.

#### 4.20 Statistical Analysis

The results were expressed as the mean±S.D.. The significance of differences was analyzed by one-way ANOVA followed by the Bonferroni correction. A value of  $P < 0.05$  was considered statistically significant.

## Declarations

**Supporting information** UV absorption spectrum of AcAs (100 μM), <sup>1</sup>H NMR, <sup>13</sup>C NMR and ESI/TOF Ms spectra of AcAs and intermediates, figure and table of AcAs detected by HPLC, assignments of the observed peaks in the ESI/TOF Ms spectrum of AcAs, Molecular Formula Strings of the compounds AcAs, As and Ac, 3D PDB files of docking models for Figure 5D.

**Funding** This work was supported by the Natural Science Foundation of Jiangsu Province [Grant number BK20180570]. We are grateful to Jiangsu Province Hi-Tech Key Laboratory for Biomedical Research to support this work.

**Conflict of interest** The authors declare no conflict of interest.

**Availability of data and material** The isoenzymes and functions of carbonic anhydrase was found in Uniprot Database (<https://www.uniprot.org>). The gene expression score in Fig. 1A was found in Bgee Database (<https://bgee.org>). The protein-protein interaction in Fig. 1B and Fig. 1C was analyzed in Pathway Commons Database (<http://www.pathwaycommons.org/>) and String Database (<https://string-db.org/>), respectively.

**Code availability** Not applicable.

**Authors' contributions** GS conceived and designed the project. ZW performed the experiments with the help of ZB and FK, and ZW was a major contributor in writing the manuscript. YX provided guidance on the bioinformatics analysis. LJ performed the docking work. All authors read and approved the final manuscript.

**Ethics approval** All applicable international, national, and/or institutional guidelines for the care and use of animals were followed.

**Consent to participate** Not applicable.

**Consent for publication** Not applicable.

## References

1. Thygesen K, Alpert JS, Jaffe AS, Chaitman BR, Bax JJ, Morrow DA, White HD. Fourth universal definition of myocardial infarction (2018). *J Am Coll Cardiol.* 2019; 72 (18): 2231–2264.
2. Sharma A, Arambula JF, Koo S, Kumar R, Singh H, Sessler JL, Kim JS. Hypoxia-targeted drug delivery. *Chem Soc Rev.* 2019; 48 (3): 771–813.
3. Lan GX, Ni KY, Xu ZW, Veroneau SS, Song Y, Lin WB. Nanoscale metal-organic framework overcomes hypoxia for photodynamic therapy primed cancer immunotherapy. *J Am Chem Soc.* 2018; 140 (17): 5670–5673.
4. Raber I, McCarthy CP, Vaduganathan M, Bhatt DL, Wood DA, Cleland JGF, Blumenthal RS, McEvoy JW. The rise and fall of aspirin in the primary prevention of cardiovascular disease. *Lancet.* 2019; 393 (10186): 2155–2167.
5. Ridker PM. Should aspirin be used for primary prevention in the post-statin era? *New Engl J Med.* 2018; 379 (16): 1572–1574.
6. Chen J, Luo HL, Liu Y, Zhang W, Li HX, Luo T, Zhang K, Zhao YX, Liu JJ. Oxygen-self-produced nanoplatform for relieving hypoxia and breaking resistance to sonodynamic treatment of pancreatic cancer. *ACS Nano.* 2017; 11 (12): 12849–12862.
7. Liu JN, Bu WB, Shi JL. Chemical design and synthesis of functionalized probes for imaging and treating tumor hypoxia. *Chem Rev.* 2017; 117 (9): 6160–6224.
8. Berk M, Dean D, Drexhage H, McNeil JJ, Moylan S, O'Neil A, Davey CG, Sanna L, Maes M. Aspirin: a review of its neurobiological properties and therapeutic potential for mental illness. *Bmc Med.* 2013; 11 (1): 74.
9. Guirguis-Blake JM, Evans CV, Senger CA, O'Connor EA, Whitlock EP. Aspirin for the primary prevention of cardiovascular events: a systematic evidence review for the US preventive services task force. *Ann Intern Med.* 2016; 164 (12): 804–13.

10. McNeil JJ, Wolfe R, Woods RL, Tonkin AM, Donnan GA, Nelson MR, Reid CM, Lockery JE, Kirpach B, Storey E, Shah RC, Williamson JD, Margolis KL, Ernst ME, Abhayaratna WP, Stocks N, Fitzgerald SM, Orchard SG, Trevaks RE, Beilin LJ, Johnston CI, Ryan J, Radziszewska B, Jelinek M, Malik M, Eaton CB, Brauer D, Cloud G, Wood EM, Mahady SE, Satterfield S, Grimm R, Murray AM. Effect of aspirin on cardiovascular events and bleeding in the healthy elderly. *New Engl J Med*. 2018; 379 (16): 1509–1518.
11. Packer M. Critical examination of mechanisms underlying the reduction in heart failure events with SGLT2 inhibitors: identification of a molecular link between their actions to stimulate erythrocytosis and to alleviate cellular stress. *Cardiovasc Res*. 2020; 117 (1): 74–84.
12. Semenza GL, Mechanisms of disease oxygen sensing, homeostasis, and disease. *New Engl J Med*. 2011; 365 (10): 537–547.
13. (13) Cao Q, Zhou DJ, Pan ZY, Yang GG, Zhang H, Ji LN, Mao ZW. CAIXplatins: highly potent Pt(IV) prodrugs selectively against hypoxic tumors via microenvironment and metabolism regulation. *Angew Chem Int Edit*. 2020; 59 (42): 18556–18562.
14. (14) Cui J, Zhang Q, Song Q, Wang HR, Dmitriev P, Sun MY, Cao XY, Wang Y, Guo LM, Indig IH, Rosenblum JS, Ji CX, Cao DQ, Yang KY, Gilbert MR, Yao Y, Zhuang ZP. Targeting hypoxia downstream signaling protein, CAIX, for CAR T-cell therapy against glioblastoma. *Neuro-Oncology*. 2019; 21 (11): 1436–1446.
15. (15) John A, Sivashanmugam M, Natarajan SK, Umashankar V. Computational modeling of novel inhibitory peptides targeting proteoglycan like region of carbonic anhydrase IX and in vitro validation in HeLa cells. *J Biomol Struct Dyn*. 2020; 38 (7): 1995–2006.
16. (16) Jung HS, Han J, Shi H, Koo S, Singh H, Kim HJ, Sessler JL, Lee JY, Kim JH, Kim JS. Overcoming the limits of hypoxia in photodynamic therapy: a carbonic anhydrase IX-targeted approach. *J Am Chem Soc*. 2017; 139 (22): 7595–7602.
17. (17) Scheibe RJ, Gros G, Parkkila S, Waheed A, Grubb JH, Shah GN, Sly WS, Wetzel P. Expression of membrane-bound carbonic anhydrases IV, IX, and XIV in the mouse heart. *J Histochem CytoChem*. 2006; 54 (12): 1379–1391.
18. (18) Vargas LA, Pinilla OA, Diaz RG, Sepulveda DE, Swenson ER, Perez NG, Alvarez BV. Carbonic anhydrase inhibitors reduce cardiac dysfunction after sustained coronary artery ligation in rats. *Cardiovasc Pathol*. 2016; 25 (6): 468–477.
19. (19) Orlowski A, De Giusti VC, Morgan PE, Aiello EA, Alvarez BV. Binding of carbonic anhydrase IX to extracellular loop 4 of the NBCe1  $\text{Na}^+/\text{HCO}_3^-$  cotransporter enhances NBCe1-mediated  $\text{HCO}_3^-$  influx in the rat heart. *Am J Physiol-Cell Ph*. 2012; 303 (1): C69–80.
20. (20) Robertson N, Potter C, Harris AL. Role of carbonic anhydrase IX in human tumor cell growth, survival, and invasion. *Cancer Res*. 2004; 64 (17): 6160–6165.
21. (21) Kim JW, Tchernyshyov I, Semenza GL, Dang CV. HIF-1-mediated expression of pyruvate dehydrogenase kinase: A metabolic switch required for cellular adaptation to hypoxia. *Cell Metab*. 2006; 3 (3): 177–185.

22. (22) Takov K, He ZH, Johnston HE, Timms JF, Guillot PV, Yellon DM, Davidson SM. Small extracellular vesicles secreted from human amniotic fluid mesenchymal stromal cells possess cardioprotective and promigratory potential. *Basic Res Cardiol.* 2020; 115 (3): 26.
23. (23) He Y, Zhou LY, Fan ZQ, Liu SK, Fang WJ. Palmitic acid, but not high-glucose, induced myocardial apoptosis is alleviated by N-acetylcysteine due to attenuated mitochondrial-derived ROS accumulation-induced endoplasmic reticulum stress. *Cell Death Dis.* 2018; 9 (5): 568.
24. (24) Zhao YP, Wang F, Jiang W, Liu JF, Liu BL, Qi LW, Zhou W, A mitochondrion-targeting tanshinone IIA derivative attenuates myocardial hypoxia reoxygenation injury through a SDH-dependent antioxidant mechanism. *J Drug Target.* 2019; 27 (8): 896–902.
25. (25) Levey AS, Stevens LA, Schmid CH, Zhang YP, Castro AF, Feldman HI, Kusek JW, Eggers P, Van Lente F, Greene T. A new equation to estimate glomerular filtration rate. *Ann Intern Med.* 2009; 150 (9): 604–612.
26. (26) Morris GM, Goodsell DS, Halliday RS, Huey R, Hart WE, Belew RK, Olson AJ. Automated docking using a lamarckian genetic algorithm and an empirical binding free energy function. *J Comput Chem.* 1998; 19 (14): 1639–1662.
27. (27) Wan F g, Peng QQ, Liu JF, Alolga RN, Zhou W. A novel ferulic acid derivative attenuates myocardial cell hypoxia reoxygenation injury through a succinate dehydrogenase dependent antioxidant mechanism. *Eur J Pharmacol.* 2019; 856: 172417.
28. (28) Osadchii OE. Cardiac hypertrophy induced by sustained beta-adrenoreceptor activation: pathophysiological aspects. *Heart Fail Rev.* 2007; 12: 66–86.
29. (29) Allawadhi P, Khurana A, Sayed N, Kumari P, Godugu C. Isoproterenol-induced cardiac ischemia and fibrosis: Plant-based approaches for intervention. *Phytother Res.* 2018; 32 (10): 1908–1932.

## Tables

**Table 1** Effect of AcAs and As on CK-MB activity and cTNI level in ISO treated myocardial ischemia injury mice.

	CK-MB (U/L)	cTNI (pg/mL)
Blank	97.0 ± 10.1	28.9 ± 5.2
Model	313.4 ± 32.8	1453.6 ± 376.6
AcAs	116.9 ± 23.3	516.5 ± 90.4
As	267.2 ± 37.1	871.7 ± 102.9

## Figures

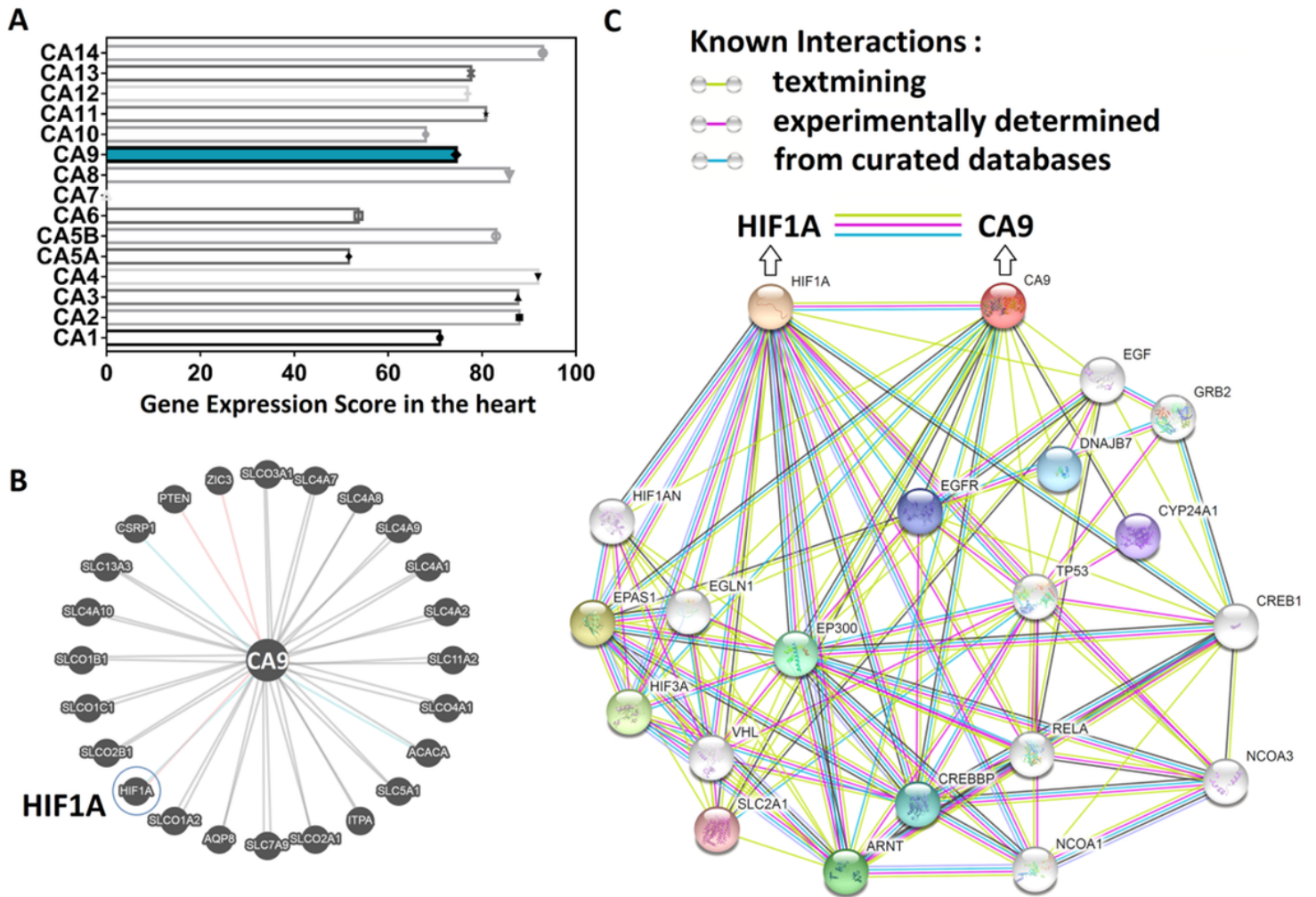


**Figure 1**

Protein distribution of carbonic anhydrase isoenzymes in the heart (A) and protein-protein interaction between CAIX and HIF-1 $\alpha$  (A: Bgee Database; B: Pathway Commons Database; C: String Database).

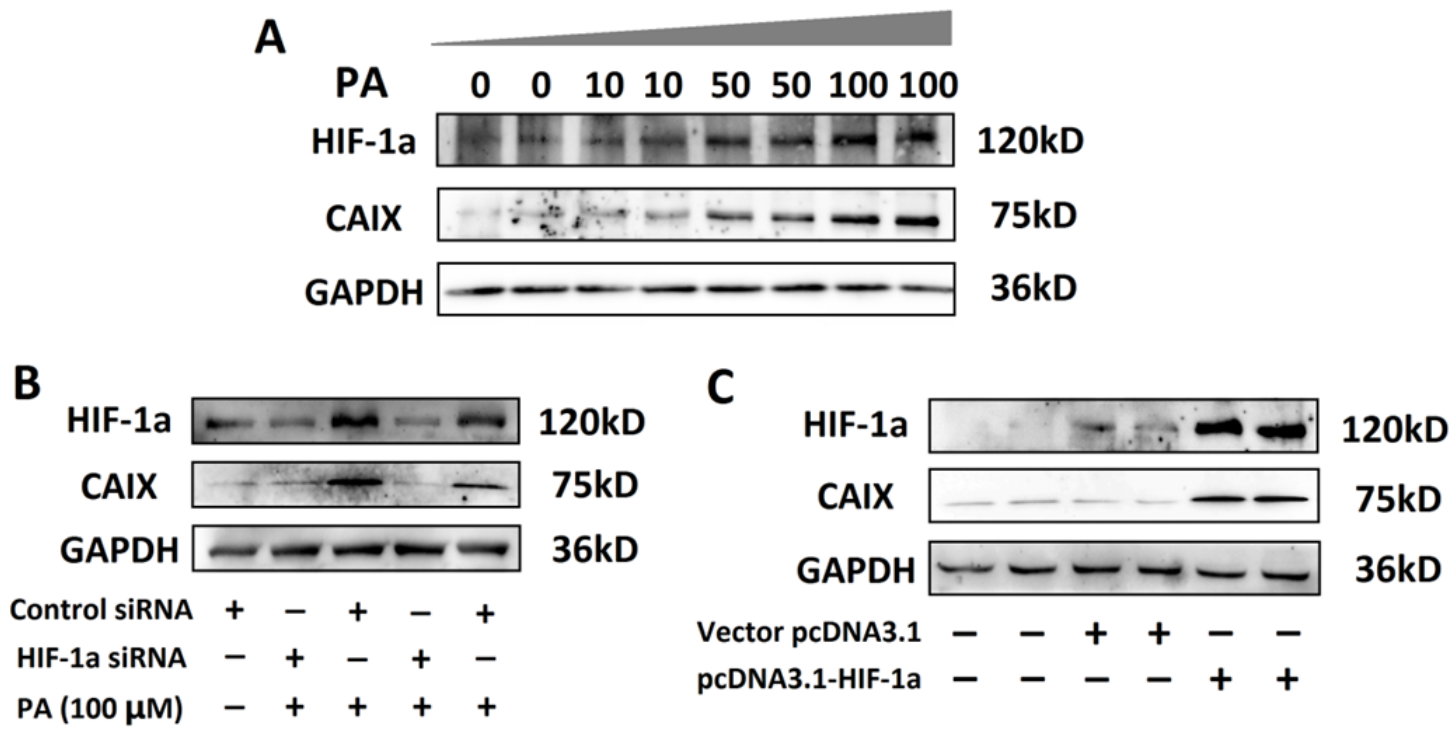


**Figure 2**

A. HIF-1α and CAIX protein expression in H9c2 cells treated with palmitic acid (PA) (0–100 μM) for 4 h; B. HIF-1α and CAIX expression in H9c2 cells transfected with HIF-1α or control scrambled siRNAs; C. HIF-1α and CAIX expression in H9c2 cells transfected with pcDNA3.1-HIF-1α or vehicle. The results were expressed as the mean±SD of three independent experiments.

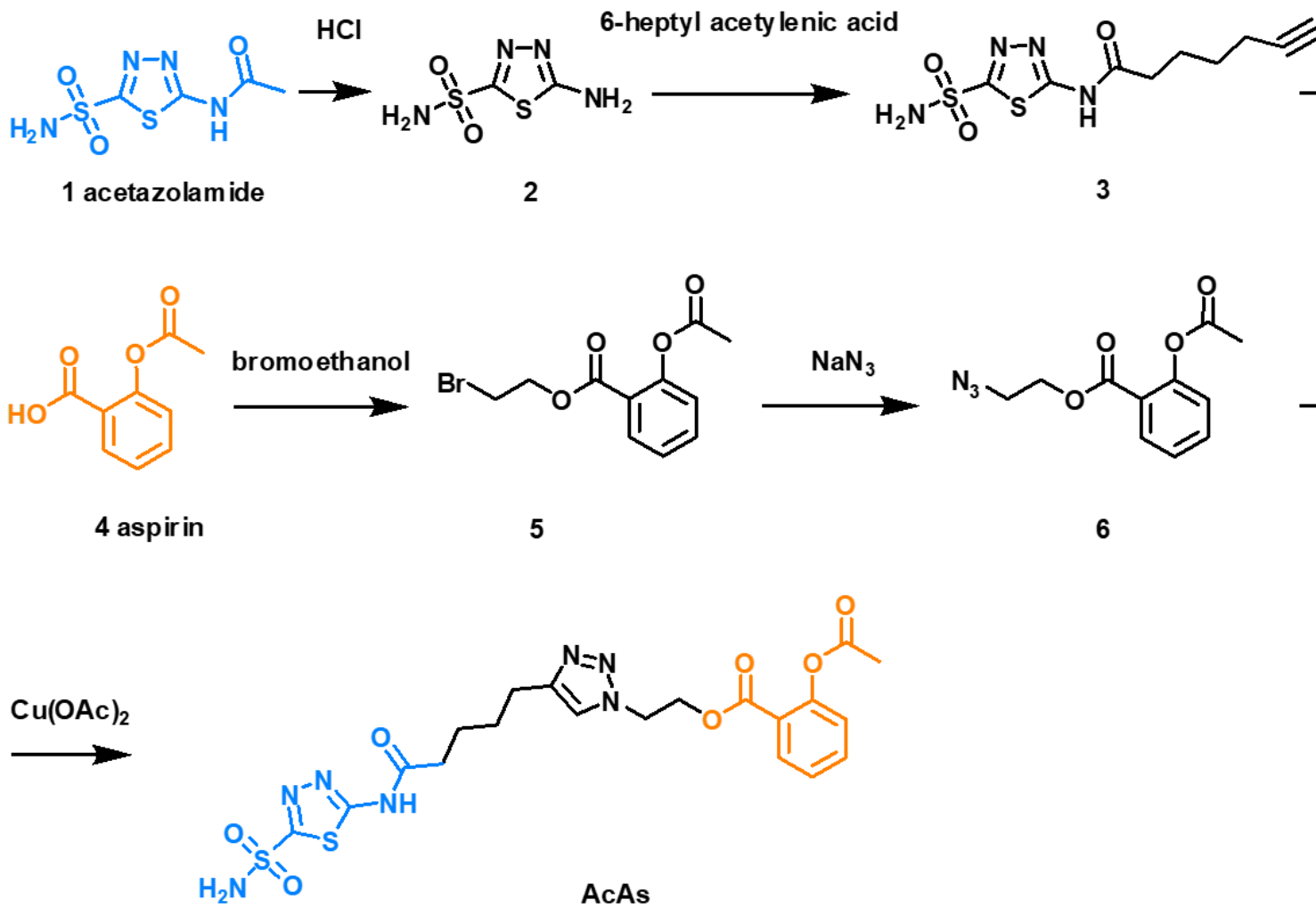


Figure 3

Synthetic way of preparing the target compound AcAs.

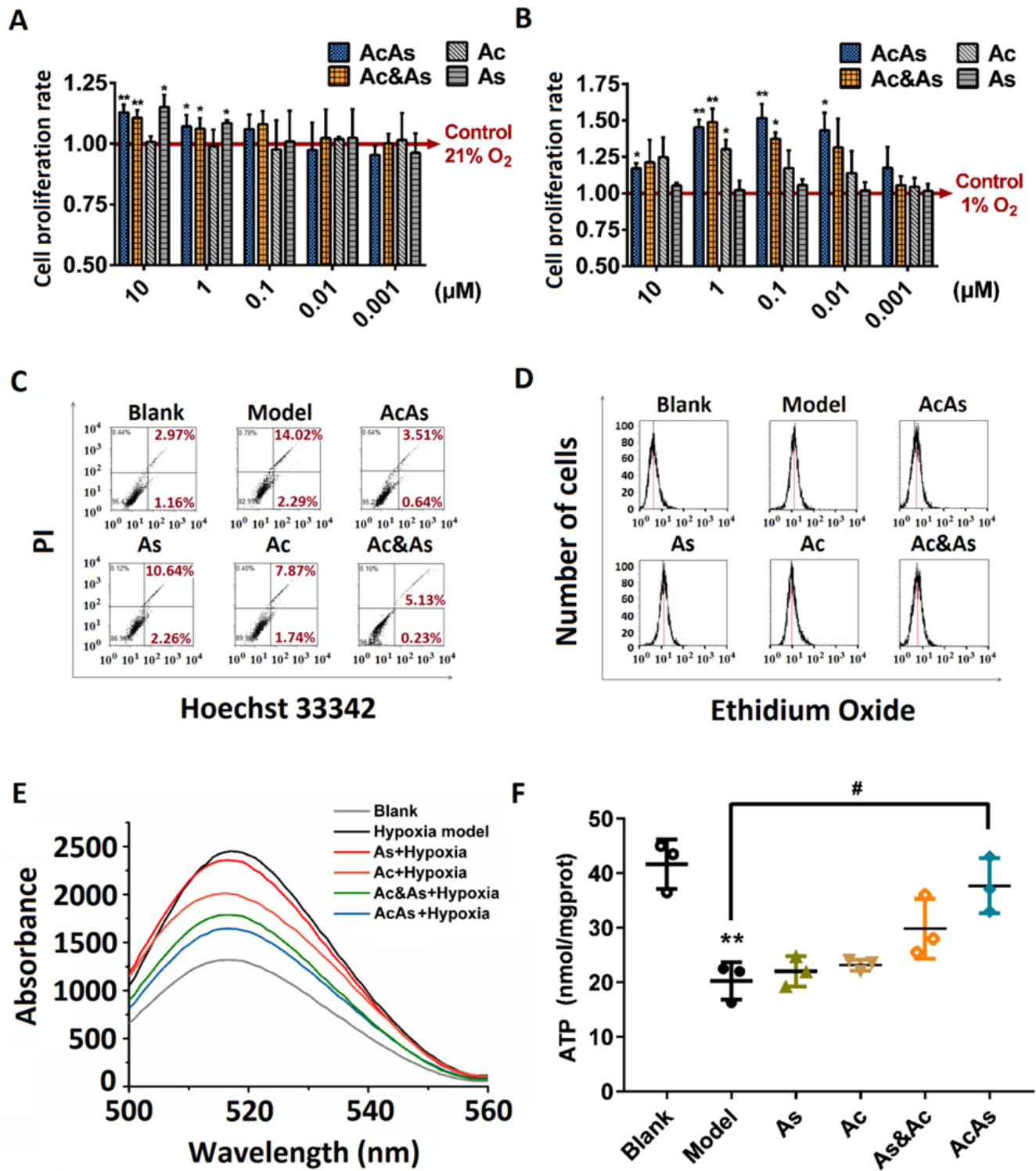


Figure 4

Cell proliferation influenced by As, Ac, AcAs or a combined use of Ac and As (Ac&As) (0.001–10  $\mu\text{M}$ ), respectively under 21% or 1% oxygen conditions. Data were expressed as the mean $\pm$ SD from three independent experiments. \* $p$ <0.05, \*\*<0.01 versus the group without drug (A. 1% O<sub>2</sub> Model group, B. 21% O<sub>2</sub> Blank group). C. H9c2 cell membrane integrities of blank group, model group (1% O<sub>2</sub>) and medicated groups (10  $\mu\text{mol/L}$  As, Ac, AcAs or Ac&As under 1% O<sub>2</sub>, respectively). D. Cell distribution of H9c2 cells

under different fluorescence intensities of DCF in blank group, model group (1% O<sub>2</sub>) and medicated groups (1% O<sub>2</sub> and 10 μM As, Ac, AcAs or Ac&As, respectively). E. ROS regulatory effect of As, Ac, AcAs or Ac&As (10 μM) for hypoxia treated H9c2 cells (DHE oxide, λ<sub>ex</sub>=488 nm, λ<sub>em</sub>=520 nm). F. ATP regulation effect of As, Ac, AcAs or Ac&As for hypoxia treated H9c2 cells. Data were expressed as the mean±SD from three independent experiments. \*\*p<0.01: model group vs blank group; #p<0.05: AcAs medicated group vs model group.

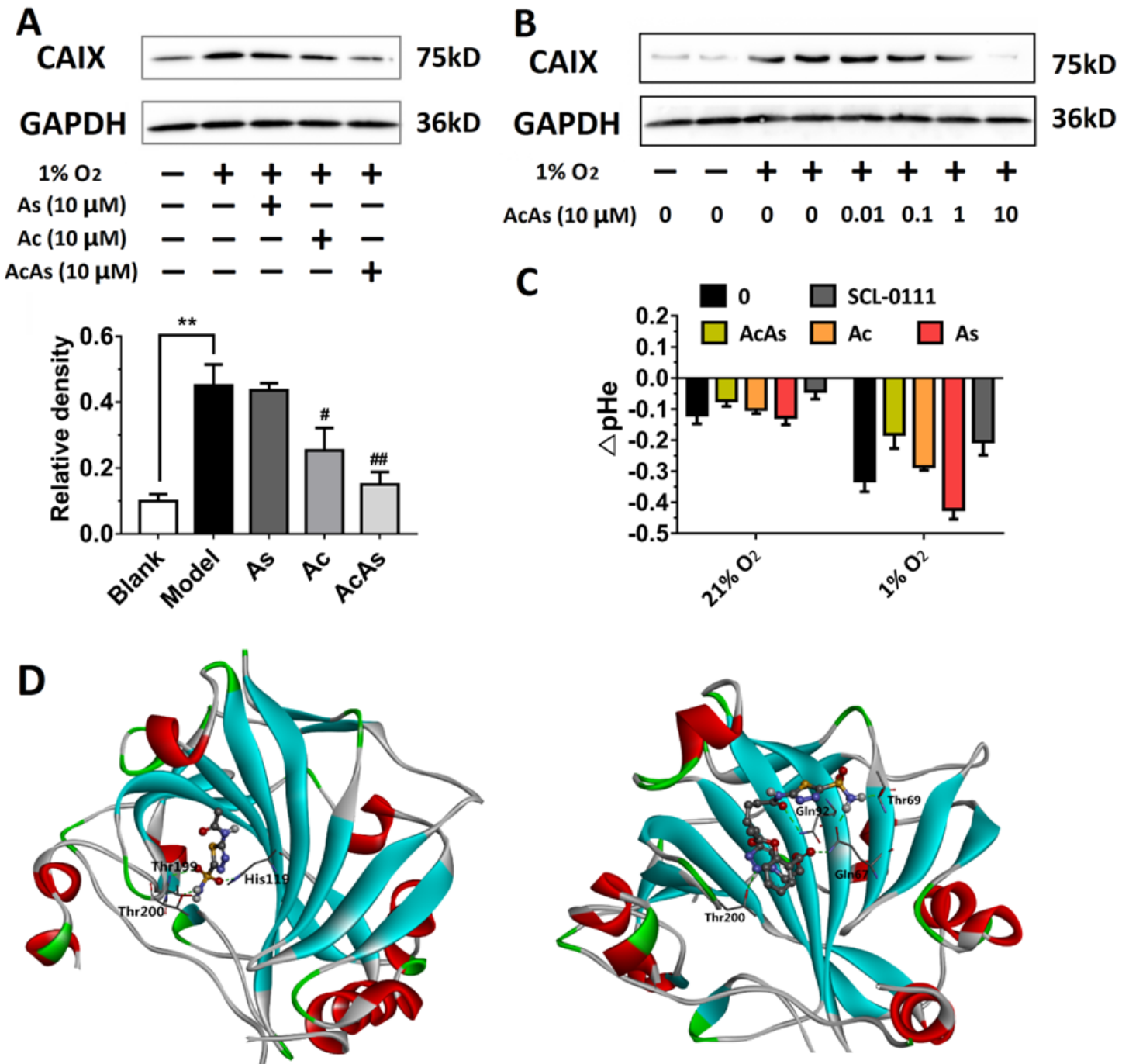
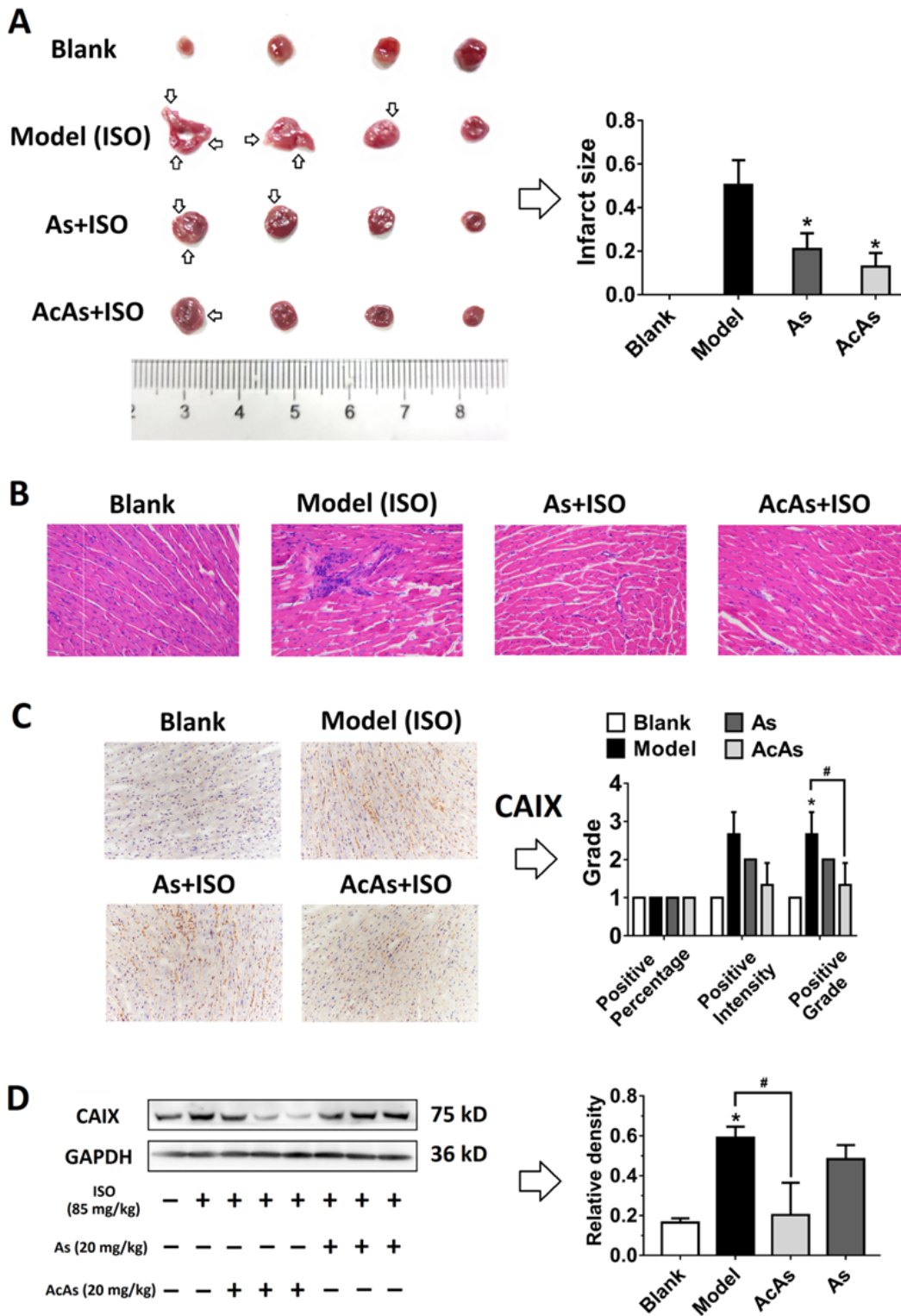


Figure 5

A. CAIX protein expression in H9c2 cells in response to hypoxia modeling with or without As, Ac, AcAs, respectively. B. CAIX protein expression in H9c2 cells in response to hypoxia modeling with or without

0.01–10  $\mu$ M AcAs, respectively. C Impact of Ac, As, AcAs, SLC-0111 on extracellular pH values of H9c2 cells. D. The best docking mode between Ac or AcAs and amino acid residues around the active site of CAIX (PDB ID: 6FE2).



**Figure 6**

A. Macroscopic enzyme mapping assays (TTC test) of mouse heart tissues in blank, model (85 mg/kg ISO) and medicated groups (20 mg/kg As+85 mg/kg ISO, 20 mg/kg AcAs+85 mg/kg ISO). Six mice in

each group were used. B. Effect of pretreatment with As or AcAs on pathological changes in ISO induced myocardial ischemia injury mice model. C. Immunohistochemistry examinations of CAIX accumulation in mice heart. D. CAIX protein expression in myocardial tissue in response to ISO treatment with or without As, AcAs, respectively.

## Supplementary Files

This is a list of supplementary files associated with this preprint. Click to download.

- [Graphicformanuscript.docx](#)
- [SupplementaryInformation.docx](#)